J. Am. Chem. Soc. 1992, 114, 3341–3346

Polyoxo Alkoxides of Vanadium: The Structures of the Decanuclear Vanadium(IV) Clusters $[V_{10}O_{16}\{CH_3CH_2C(CH_2O)_3\}_4]^{4-}$ and $[V_{10}O_{13}\{CH_3CH_2C(CH_2O)_3\}_5]^-$

M. Ishaque Khan,[†] Qin Chen,[†] D. P. Goshorn,[‡] Hakon Hope,[§] Sean Parkin,[§] and Jon Zubieta*,[†]

Contribution from the Department of Chemistry, Syracuse University, Syracuse, New York 13244-4100, Department of Chemistry, University of California, Davis, California 95616, and Exxon Research and Engineering Company, Annandale, New Jersey 08801. *Received August 30, 1991*

Abstract: The hydrothermal reaction of a mixture of vanadium oxides with $CH_3CH_2C(CH_2OH)_3$ in the presence of NH_4Cl yields $(NH_4)_4[V_{10}O_{16}\{CH_3CH_2C(CH_2O)_3\}_4]\cdot 4H_2O$ (I). In contrast, the reaction of vanadium oxides with the same ligand, using Et_4NCl as mineralizer, yields $(Et_4N)[V_{10}O_{13}\{CH_3CH_2C(CH_2O)_3\}_5]$ (II). Both I and II exhibit structures based on the decavanadium core, $\{V_{10}O_{28}\}$. While 12 doubly and triply bridging oxo groups of the $[V_{10}O_{28}]^{6-}$ prototype are replaced by alkoxy oxygens of the ligands in I, 15 doubly and triply bridging oxo groups are replaced in II. In addition to the incorporation of alkoxy ligands into the $\{V_{10}O_{28}\}$ core, I and II are unusual in that the vanadium sites exhibit the V(IV) oxidation state rather than V(V) as observed for the parent core. The relatively small structural distortions associated with this reduction of the core are noteworthy. Crystal data for $(NH_4)_4[V_{10}O_{16}\{CH_3CH_2C(CH_2O)_3\}_4]\cdot 4H_2O$ (I): space group, $C2/c$; $a = 17.320$ (2) Å; $b = 24.904$ (3) Å; $c = 12.430$ (2) Å; $\beta = 106.32$ (1)°; $V = 5146$ (3) Å^3; $Z = 2$; D(calc) = 1.840 g/cm^3; structure solution and refinement based on 4053 reflections, $R = 0.042$. Crystal data for $(Et_4N)[V_{10}O_{13}\{CH_3CH_2C(CH_2O)_3\}_5]$ (II): space group, $P2_1/c$; $a = 12.290$ (2) Å; $b = 19.115$ (2) Å; $c = 23.701$ (4) Å; $\beta = 98.80$ (1)°; $V = 5502$ (2) Å^3; $Z = 4$; D(calc) = 1.815 g/cm^3; 4436 reflections, $R = 0.079$. An analogous compound to II, $(Me_4N)_{2/3}(Et_4N)_{1/3}[V_{10}O_{13}\{CH_3C(CH_2O)_3\}_5]\cdot 0.69H_2O$ (III) was prepared in a similar fashion. Crystal data for $(Me_4N)_{2/3}(Et_4N)_{1/3}[V_{10}O_{13}\{CH_3C(CH_2O)_3\}_5]\cdot 0.69H_2O$ (III): space group, $P2_1/n$; $a = 12.235$ (2) Å; $b = 22.484$ (6) Å; $c = 53.439$ (13) Å; $\beta = 92.61$ (2)°; $V = 14685$ (6) Å^3; $Z = 12$; D(calc) = 1.913 g/cm^3; 11 994 reflections, $R = 0.0851$.

Introduction

While the chemistry of the "oxidized" polyoxometalates (nd^0 configuration of the metal centers) has been extensively studied,[1,2] polyoxoanions with reduced metal centers have only recently received much attention.[1,3-9] The V(IV)-containing polyoxoanions have been shown to exhibit nearly all ratios of V(IV) to V(V): from two V(IV) d^1 centers in $[AsV_{14}O_{40}]^{7-}$[9b] to eighteen V(IV) centers in $[V_{18}O_{42}H_4I]^{9-}$.[10] In the course of our investigations of the emerging structural class of oxoalkoxymolybdate and -vanadate oligomers,[11-15] we have described a series of hexavanadium clusters of nearly identical structure but with different electron populations and protonation sites as well as different types of spin–spin interactions, namely, $[V_6O_{13-n}(OH)_n\{RC(CH_2O)_3\}_2]^{2-}$ with $n = 2$, 4, and 6.[16,17] In an effort to extend this chemistry to other polyoxoalkoxyvanadium cluster types, we have sought to exploit hydrothermal synthesis in the preparation of clusters incorporating simple organic ligands. Although hydrothermal synthesis has been recently demonstrated to give numerous unusual polyoxomolybdates and polyoxovanadates of phosphorus with reduced metal centers,[18,19] this work represents the first example to our knowledge of the applications of the technique in the synthesis of coordination complexes of polyoxometalates with common organic ligands.

Experimental Section

Reagent grade chemicals were used throughout. Vanadium(III) oxide (Aldrich), vanadium(V) oxide (Aldrich), ammonium metavanadate (Alfa), 1,1,1-tris(hydroxymethyl)ethane (Aldrich), 1,1,1-tris(hydroxymethyl)propane (Fluka), tetramethylammonium chloride (Aldrich), tetramethylammonium bromide (Aldrich), and ammonium chloride were used as received from the commercial sources.

Preparation of $(NH_4)_4[V_{10}O_{16}\{CH_3CH_2C(CH_2O)_3\}_4]\cdot 4H_2O$ (I). Vanadium(III) oxide, ammonium metavanadate, 1,1,1-tris(hydroxymethyl)propane, ammonium chloride, and water in the mole ratio 3:6:10:5:300 were placed in a Parr Teflon-lined acid digestion bomb. After being heated for 20 h in a Thermolyne electric furnace at 150 °C, the mixture was allowed to cool to room temperature. Large black

---

[†] Syracuse University.
[‡] Exxon Research and Engineering Co.
[§] University of California, Davis.

(1) Pope, M. T.; Müller, A. *Angew. Chem. Int. Ed. Engl.* **1991**, *30*, 34. Pope, M. T. In *Comprehensive Coordination Chemistry*; Wilkinson, G., Gillard, R. D., McCleverty, J. A., Eds.; Pergamon: Oxford, U.K., 1987; Vol. 3, p 1023. Pope, M. T. *Heteropoly and Isopoly Oxometalates*; Springer: New York, 1983.

(2) Day, V. W.; Klemperer, W. G. *Science (Washington, D.C.)* **1985**, *228*, 533.

(3) Müller, A.; Döring, J.; Bögge, H. *J. Chem. Soc., Chem. Commun.* **1991**, 273.

(4) Müller, A.; Döring, J.; Khan, M. I.; Wittenben, V. *Angew. Chem., Int. Ed. Engl.* **1991**, *30*, 210.

(5) Müller, A.; Krickemeyer, E.; Penk, M.; Wittenben, V.; Döring, J. *Angew. Chem., Int. Ed. Engl.* **1990**, *29*, 88.

(6) Müller, A.; Krickemeyer, E.; Penk, M.; Walberg, H.-J.; Bögge, H. *Angew. Chem., Int. Ed. Engl.* **1987**, *26*, 1045.

(7) Müller, A.; Penk, M.; Krickemeyer, E.; Bögge, H.; Walberg, H.-J. *Angew. Chem., Int. Ed. Engl.* **1988**, *27*, 1719.

(8) Müller, A.; Döring, J. *Angew. Chem., Int. Ed. Engl.* **1988**, *27*, 174.

(9) (a) Khan, M. I.; Chen, Q.; Zubieta, J.; Goshorn, D. P.; Haushalter, R. C. *Inorg. Chim. Acta.*, in press. (b) Khan, M. I.; Müller, A. Personal communication.

(10) Müller, A.; Penk, M.; Rohlfing, R.; Krickemeyer, E.; Döring, J. *Angew. Chem., Int. Ed. Engl.* **1990**, *29*, 926.

(11) Ma, L.; Liu, S.; Zubieta, J. *J. Chem. Soc., Chem. Commun.* **1989**, 440.

(12) Ma, L.; Liu, S.; Zubieta, J. *Inorg. Chem.* **1989**, *28*, 177.

(13) Liu, S.; Ma, L.; McGowty, D.; Zubieta, J. *Polyhedron* **1990**, *9*, 1541.

(14) Chen, Q.; Liu, S.; Zubieta, J. *Inorg. Chem.* **1989**, *28*, 4433.

(15) Chen, Q.; Liu, S.; Zubieta, J. *Angew. Chem., Int. Ed. Engl.* **1990**, *29*, 70.

(16) Chen, Q.; Zubieta, J. *Inorg. Chem.* **1990**, *29*, 1458.

(17) Chen, Q.; Goshorn, D.; Scholes, C.; Tan, X.; Zubieta, J. Manuscript in preparation.

(18) Mundi, L. A.; Strohmaier, K. G.; Haushalter, R. C. *Inorg. Chem.* **1991**, *30*, 154. Haushalter, R. C.; Strohmaier, K. G.; Lai, F. W. *Science (Washington, D.C.)* **1989**, *246*, 1289. King, H. E., Jr.; Mundi, L. A.; Strohmaier, K. G.; Haushalter, R. C. *J. Solid State Chem.* **1991**, *92*, 1, 154. Haushalter, R. C.; Mundi, L. A.; Strohmaier, K. G. *J. Am. Chem. Soc.* **1990**, *112*, 8182. Haushalter, R. C.; Lai, F. W. *Angew. Chem., Int. Ed. Engl.* **1989**, *28*, 743. Mundi, L. A.; Strohmaier, K. G.; Goshorn, D. P.; Haushalter, R. C. *J. Am. Chem. Soc.* **1990**, *112*, 8182.

0002-7863/92/1514-3341$03.00/0

Table I. Crystal Data and Experimental Parameters for the X-ray Crystallographic Studies of $(NH_4)_4[V_{10}O_{16}\{CH_3CH_2C(CH_2O)_3\}_4]\cdot 4H_2O$ (I), $(Et_4N)[V_{10}O_{13}\{CH_3CH_2C(CH_2O)_3\}_5]$ (II), and $[Me_4N]_{2/3}[Et_4N]_{1/3}[V_{10}O_{13}\{CH_3C(CH_2O)_3\}_5]\cdot 0.69H_2O$ (III)

	I	II	III
	(A) Crystal Parameters		
T, K	294	294	120
a, Å	17.320 (2)	12.290 (2)	12.235 (2)
b, Å	24.904 (3)	19.115 (2)	22.484 (6)
c, Å	12.430 (2)	23.701 (4)	54.439 (13)
β, deg	106.32 (1)	98.80 (1)	92.61 (2)
V, Å	5146 (3)	5502 (2)	14685 (6)
size, mm	0.32 × 0.34 × 0.40	0.31 × 0.32 × 0.41	0.65 × 0.16 × 0.06
space group	$C2/c$	$P2_1/c$	$P2_1/n$
fw, amu	1425.5	1503.4	1412.6
Z	4	4	12
D(calc), g cm^{-3}	1.840	1.815	1.913
μ(calc), cm^{-1}	17.64	16.48	16.33
	(B) Data Measurement Parameters		
radiation	Mo Kα (λ = 0.71073 Å)	Mo Kα	Cu Kα (λ = 1.54128 Å)
2θ range, deg	0–55	0–50	0–108.5
scan type	ω	ω–2θ	ω–2θ
no. of reflcns collected	6551	10523	17938
no. of reflcns used	4053	4436	11994
R	0.042	0.079	0.0851
R_w	0.057	0.090	0.0998
GOF	1.97	1.91	1.20

crystals of I were collected by filtration, washed with water, and air-dried. The yield was 30% based on vanadium. Anal. Calcd for $C_{24}H_{68}N_4O_{32}V_{10}$: C, 20.2; H, 4.77; N, 3.93. Found: C, 20.0; H, 4.36; N, 3.71. IR (KBr pellet, cm^{-1}): 1470 (w), 1450 (m), 1400 (s), 1201 (w), 1113 (s), 1041 (vs), 972 (vs), 942 (s), 840 (s), 773 (m), 644 (sh), 613 (s), 583 (vs), 483 (s).

Preparation of $(Et_4N)[V_{10}O_{13}\{CH_3CH_2C(CH_2O)_3\}_5]$ (II). Vanadium(III) oxide, vanadium(V) oxide, 1,1,1-tris(hydroxymethyl)propane, tetraethylammonium bromide, tetramethylammonium chloride, and water in the mole ratio 2.5:2.5:5:4:4:600 were placed in a Parr Teflon-lined acid digestion bomb. After being heated for 22 h at 200 °C in an electric furnace, the mixture was allowed to cool to room temperature. Shiny black crystals of II were filtered, air-dried, and separated under a microscope from some colorless impurities (yield: 20% based on vanadium). Anal. Calcd for $C_{38}H_{75}NO_{28}V_{10}$: C, 30.4; H, 5.03; N, 0.93. Found: C, 29.9; H, 4.90; N, 1.02. IR (KBr pellet, cm^{-1}): 1470 (m), 1447 (m), 1115 (s), 1043 (vs), 979 (vs), 941 (s), 836 (m), 778 (w), 615 (s), 592 (s), 580 (s), 557 (s), 534 (w), 478 (s).

Preparation of $(Me_4N)_{2/3}(Et_4N)_{1/3}[V_{10}O_{13}\{CH_3C(CH_2O)_3\}_5]\cdot 0.69H_2O$ (III). Compound III was prepared in a fashion similar to that of II except that 1,1,1-tris(hydroxymethyl)ethane was used in place of 1,1,1-tris(hydroxymethyl)propane (yield: 25% based on vanadium). Anal. Calcd for $C_{30.33}H_{61.04}NO_{28.69}V_{10}$: C, 25.8; H, 4.32; N, 0.99. Found: C, 25.2; H, 4.12; N, 0.67. IR (KBr pellet, cm^{-1}): 1459 (m), 1399 (m), 1210 (w), 1124 (s), 1037 (vs), 1024 (vs), 980 (vs), 911 (w), 838 (s), 280 (s), 621 (s), 584 (vs), 558 (s), 534 (w), 480 (w).

X-ray Crystallographic Studies. Compounds I and II were studied using a Rigaku AFC5S diffractometer. However, compound III crystallized as thin needles, and data of sufficient quality for structure refinement could not be obtained using the sealed tube instrument. Consequently data were collected on a Siemens P3RA rotating anode diffractometer at 120 K. The crystal parameters and experimental conditions of data collection are summarized in Table I. A complete description of the crystallographic methods is given in the supplementary material.

The structures were solved by direct methods and refined by full-matrix least squares. The details of the structure solutions and refinements are presented in the supplementary material. No anomalies were encountered in the refinements of the structures. Bond lengths and angles for I and II are listed in Tables II and III, respectively. Since the structural parameters for the three independent $[V_{10}O_{13}\{CH_3C(CH_2O)_3\}_5]^-$ clusters of III are essentially identical to those of the anion of II, these data are presented only in the supplementary material.

Magnetic Susceptibility Studies. Magnetic susceptibility data for powdered samples of I and II were obtained over a temperature range of 5–300 K in an applied field of 6 kG using a Quantum Design Model MPMS SQUID Magnetometer. Magnetization isotherms at 298 and 77 K were performed to correct for the presence of ferromagnetic impurities.

Results and Discussion

Although hydrothermal synthesis has a long history of application to geochemical studies and to synthetic crystal growth,[20] its routine exploitation in conventional inorganic synthesis is a relatively recent development.[18,19,21] The reaction of V_2O_3, NH_4VO_3, $CH_3CH_2C(CH_2OH)_3$, NH_4Cl, and H_2O in the mole ratio of 3:6:10:5:300 for 20 h at 150 °C yielded black shiny crystals of $(NH_4)_4[V_{10}O_{16}\{CH_3CH_2C(CH_2O)_3\}_4]\cdot 4H_2O$ (I). The infrared spectrum of I exhibited a strong band at 1042 cm^{-1}, characteristic of ν(C–O) of the ligand, and features at 972 cm^{-1} and 840 and 777 cm^{-1} associated with ν(V–O$_t$) and ν(V–O–V), respectively. In contrast, the reaction of V_2O_3, V_2O_5, $CH_3CH_2C(CH_2OH)_3$, Et_4NBr, Me_4NCl, and H_2O in the mole ration 2.5:2.5:5:4:4:600 for 22 h at 200 °C yielded black crystals of $(Et_4N)[V_{10}O_{13}\{CH_3CH_2C(CH_2O)_3\}_5]$ (II). The infrared spectrum of II again confirmed the presence of the ligand which exhibits a strong band at 1043 cm^{-1} assigned to ν(C–O). The feature at 979 cm^{-1} is characteristic of ν(V–O$_t$) for reduced V(IV) sites, while medium intensity features at 836 and 778 cm^{-1} are tentatively assigned to ν(V–O–V).

The syntheses exhibit a marked cation dependence, such that the number of trisalkoxy ligands incorporated into the core is related to the presence of the appropriate cation. Thus, the cluster of stoichiometry 4:10 $[CH_3CH_2C(CH_2O)_3]^{3-}$:V could be isolated only as the salt of the NH_4^+ cation, while various combinations of quaternary ammonium cations R_4N^+ produced the 5:10 ligand:V stoichiometry displayed by II and III. The cation dependence is further demonstrated by the use of R_3NH^+ and Na^+ as mineralizers which results in the isolation of species with the hexavanadium core and of general composition $[V_6O_7(OH)_{12-3n}\{RC(CH_2O)_3\}_n]^{x-}$, n = 2, 3, and 4.[22] Similar cation dependencies have been demonstrated in the molybdophosphate chemistry.[18] A further synthetic requirement is the presence of reduced vanadium as V(III) in V_2O_3, in the absence of which only amorphous materials are obtained.

The structures of the molecular anions of both I and II, shown in Figures 1 and 2, respectively, possess the gross metal–oxygen framework of the $[V_{10}O_{28}]^{6-}$ parent structure and the protonated ions $[H_nV_{10}O_{28}]^{(n-6)-}$, n = 2 and 3.[23-25] In the structure of Ia,

---

(19) Huan, G.; Day, V. W.; Jacobson, A. J.; Goshorn, D. P. *J. Am. Chem. Soc.* **1991**, *113*, 3188. Huan, G.; Greaney, M. A.; Jacobson, A. J. *J. Chem. Soc., Chem. Commun.* **1991**, 260. Huan, G.; Jacobson, A. J.; Day, V. W. *Angew. Chem., Int. Ed. Engl.* **1991**, *30*, 4.

(20) Laudise, R. A. *Sci. Eng. News* **1987** (Sept 28), 30.

(21) Liao, J.-H.; Kanatzidis, M. G. *J. Am. Chem. Soc.* **1990**, *112*, 7400.

(22) Khan, I.; Chen, Q.; Goshorn, D.; Zubieta, J. Manuscript in preparation.

(23) Evans, H. T. *Inorg. Chem.* **1984**, *23*, 501.

(24) Capparelli, M. V.; Goodgame, D. M. L.; Hayman, P. B.; Skapski, A. C. *J. Chem. Soc., Chem. Commun.* **1986**, 776.

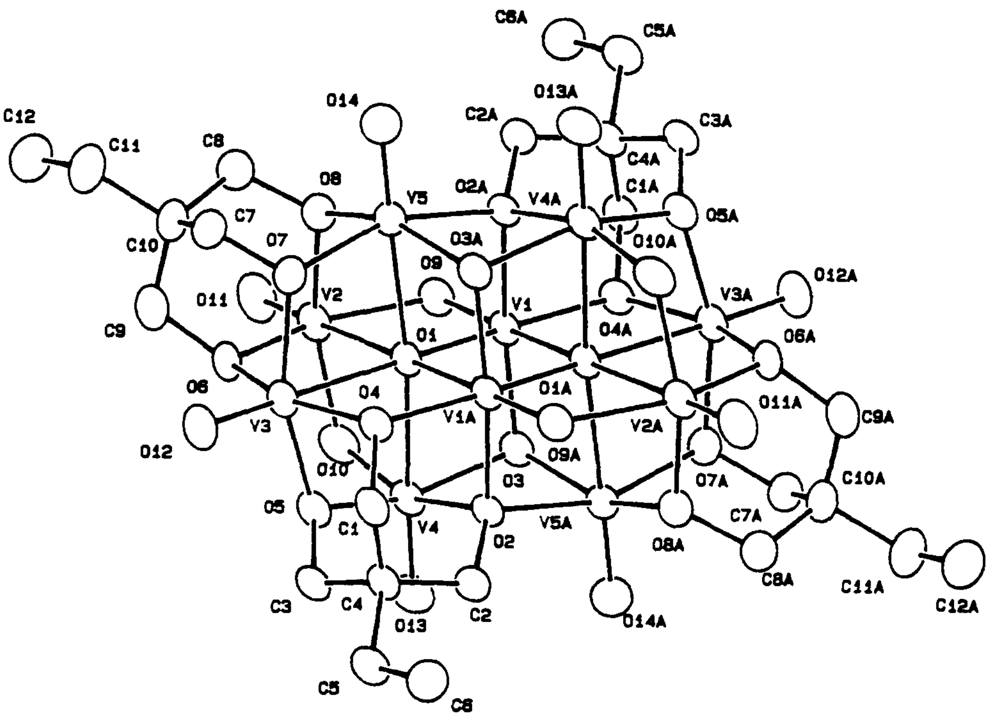

Figure 1. ORTEP view of the structure of $[V_{10}O_{16}\{CH_3CH_2C(CH_2O)_3\}_4]^{4-}$ (Ia).

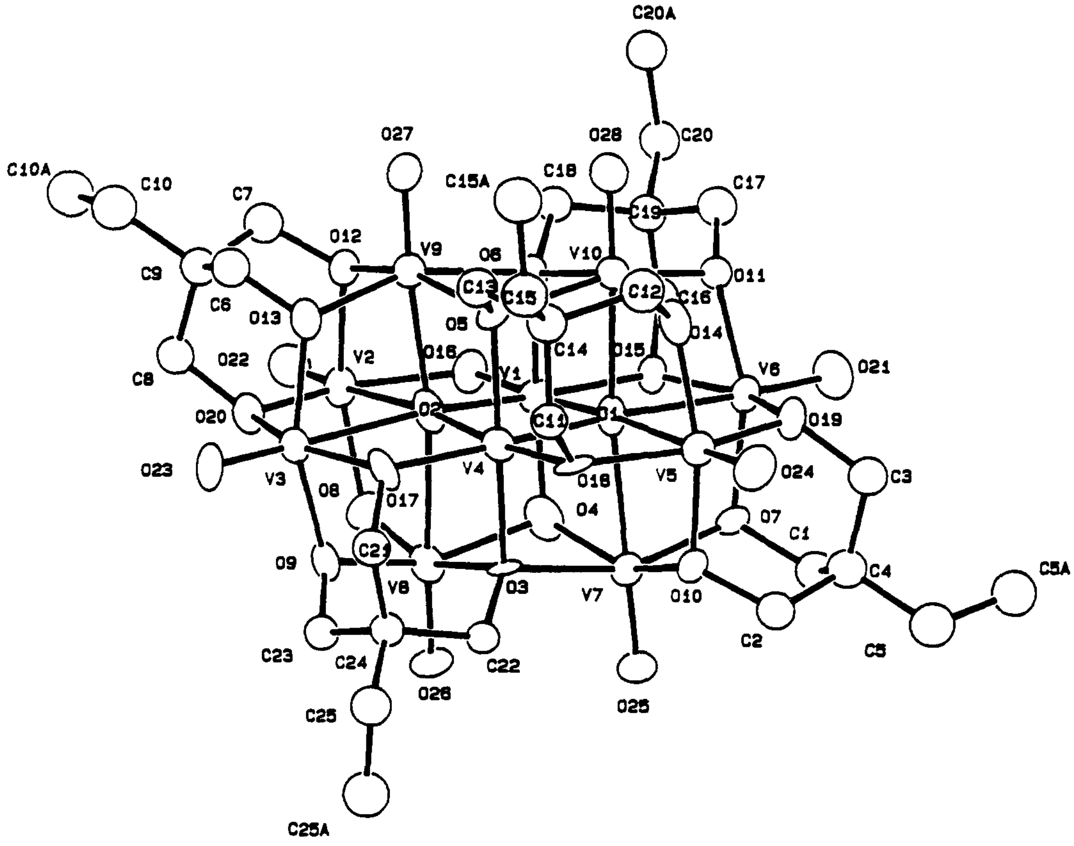

Figure 2. ORTEP view of the structure of $[V_{10}O_{13}\{CH_3CH_2C(CH_2O)_3\}_5]^{-}$ (IIa).

the molecular anion of I, ten doubly bridging oxo groups and two triply bridging oxo groups of this parent $\{V_{10}O_{28}\}$ core have been replaced by twelve alkoxy donors from the four trisalkoxy ligands.

The pattern of substitution adopted by the triols of this structure is dictated by the bonding requirements of the ligands which will bridge between three metals in a triangulo arrangement, when possible. The ligands will, therefore, tend to cap the triangular faces of the tetrahedral cavities of the decametalate framework, shown in Figure 3. Although there are twelve of these sites associated with the cluster, only six may be occupied by bridging tridentate ligands, as indicated by the highlighting. While only four possible sites are occupied in the structure of Ia, there is no a priori reason that further substitution will not occur. By appropriate cation selection, the 5:10 ligand:V cluster, $[V_{10}O_{13}\{CH_3CH_2C(CH_2O)_3\}_5]^{1-}$ (IIa), was isolated, confirming that

---

(25) Day, V. W.; Klemperer, W. G.; Maltbie, D. J. *J. Am. Chem. Soc.* **1987**, *109*, 2991.

Table II. Selected Bond Lengths (Å) and Angles (deg) for $(NH_4)_4[V_{10}O_{16}\{CH_3CH_2C(CH_2O)_3\}_4]\cdot 4H_2O$ (I)

V1–O1	2.014 (3)	V4–O13	1.589 (4)
V1–O1	2.140 (3)	V5–O1	2.351 (3)
V1–O2	2.077 (3)	V5–O2	2.068 (3)
V1–O3	1.935 (3)	V5–O3	1.981 (3)
V1–O4	1.968 (3)	V5–O7	1.991 (3)
V1–O9	1.656 (3)	V5–O8	2.007 (3)
V2–O1	2.447 (3)	V5–O14	1.587 (4)
V2–O6	1.994 (3)	V3–O6	2.000 (3)
V2–O8	1.995 (3)	V3–O7	1.997 (3)
V2–O9	2.017 (3)	V3–O12	1.599 (3)
V2–O10	1.971 (4)	V4–O1	2.407 (3)
V2–O11	1.586 (3)	V4–O2	2.135 (3)
V3–O1	2.322 (3)	V4–O3	1.933 (3)
V3–O4	2.012 (3)	V4–O5	1.966 (3)
V3–O5	2.004 (3)	V4–O10	1.813 (3)
O1–V1–O2	85.9 (1)	O5–V3–O7	159.6 (1)
O1–V1–O3	87.0 (1)	O5–V3–O12	100.2 (2)
O1–V1–O4	166.5 (1)	O6–V3–O7	88.6 (1)
O1–V1–O9	92.5 (1)	O6–V3–O12	100.4 (2)
O2–V1–O3	162.6 (1)	O7–V3–O12	100.3 (2)
O2–V1–O4	88.6 (1)	O1–V4–O2	74.7 (1)
O2–V1–O9	94.6 (1)	O1–V4–O3	76.7 (1)
O3–V1–O4	94.7 (1)	O1–V4–O5	77.9 (1)
O3–V1–O9	101.5 (1)	O1–V4–O10	81.5 (1)
O4–V1–O9	100.3 (1)	O1–V4–O13	173.4 (2)
O1–V2–O6	79.1 (1)	O2–V4–O3	77.3 (1)
O1–V2–O8	77.8 (1)	O2–V4–O5	83.2 (1)
O1–V2–O9	72.5 (1)	O2–V4–O10	156.2 (1)
O1–V2–O10	77.5 (1)	O2–V4–O13	99.1 (2)
O1–V2–O11	178.0 (2)	O3–V4–O5	151.3 (1)
O6–V2–O8	87.1 (1)	O3–V4–O10	97.4 (1)
O6–V2–O9	151.6 (1)	O3–V4–O13	104.2 (2)
O6–V2–O10	86.8 (1)	O5–V4–O10	91.9 (1)
O6–V2–O11	102.9 (2)	O5–V4–O13	99.6 (2)
O8–V2–O9	86.8 (1)	O10–V4–O13	104.8 (2)
O8–V2–O10	155.2 (1)	O1–V5–O2	78.0 (1)
O8–V2–O11	102.8 (2)	O1–V5–O3	75.4 (1)
O9–V2–O10	87.3 (1)	O1–V5–O7	79.7 (1)
O9–V2–O11	105.5 (2)	O1–V5–O8	79.9 (1)
O10–V2–O11	102.0 (2)	O1–V5–O14	178.5 (2)
O1–V3–O4	77.7 (1)	O2–V5–O3	77.9 (1)
O1–V3–O5	79.3 (1)	O2–V5–O7	157.5 (1)
O1–V3–O6	82.1 (1)	O2–V5–O8	91.9 (1)
O1–V3–O7	80.3 (1)	O2–V5–O14	100.5 (2)
O1–V3–O12	177.4 (2)	O3–V5–O7	93.3 (1)
O4–V3–O5	86.9 (1)	O3–V5–O8	154.7 (1)
O4–V3–O6	159.9 (1)	O3–V5–O14	103.9 (2)
O4–V3–O7	88.7 (1)	O7–V5–O8	87.4 (1)
O4–V3–O12	99.7 (2)	O7–V5–O14	101.7 (2)
O5–V3–O6	88.8 (1)	O8–V5–O14	100.7 (2)

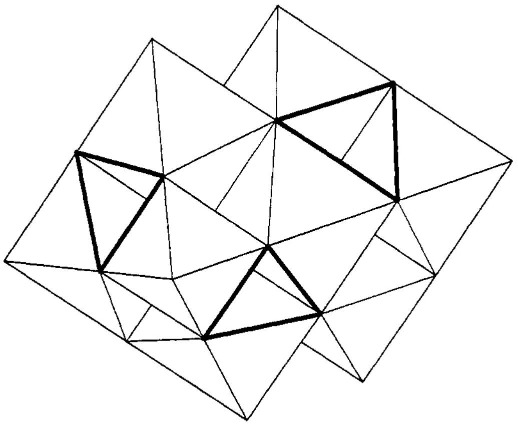

Figure 3. Schematic representation of the $\{V_{10}O_{28}\}$ core, viewed as edge-sharing octahedra. The triangular faces available for occupation by trisalkoxy oxygen donors are highlighted.

variable stoichiometries of ligand to metal may be achieved.

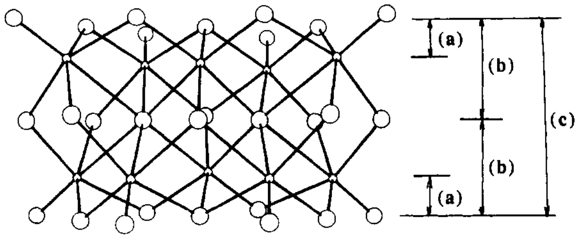

Figure 4. Schematic representation of the $\{V_{10}O_{28}\}$ core, viewed as layers of negatively charged oxygen atoms with intervening layers of vanadium atoms. Interplanar distances are defined by *a*, *b*, and *c* and values are provided in Table IV.

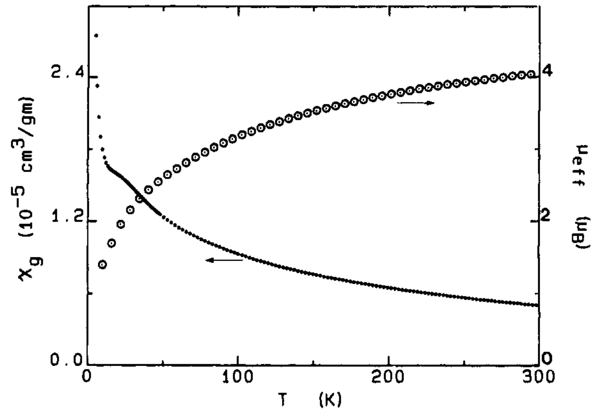

Figure 5. Plot of the magnetic susceptibility (χ_g) and effective moment (μ_{eff}) per molecule for solid I.

That a maximum of five site occupation by the trisalkoxy ligands has been achieved may suggest that occupancy of the sixth site, with concomitant change in the cluster charge to +2, results in unfavorable electrostatics. Attempts to isolate the $[V_{10}O_{10}\{RC(CH_2O)_3\}_6]^{2+}$ clusters have invariably led to $[V_6O_7\{RC(CH_2O)_3\}_4]^{2-}$ cluster types.[22]

An unusual feature of the structure is the presence of vanadium exclusively in the reduced form, d^1 V(IV), an observation consistent both with the charge requirements of the cluster and with valence sum calculations[26] on the vanadium centers, which yield bond numbers in the range of 3.9–4.1 valence units for all vanadium sites of I–III. Some distortion of the $\{V_{10}O_{28}\}$ core of I–III from that of the parent cluster $[V_{10}O_{28}]^{6-}$ would be anticipated. The structural consequences of reduction and ligation on the $\{V_{10}O_{28}\}$ core are illustrated in Figure 4 and Table IV, which compare the spacings between approximately planar layers of negatively charged, close-packed oxygen atoms separated by layers of cationic vanadium centers for $[V_{10}O_{28}]^{6-}$, $[H_3V_{10}O_{28}]^{3-}$, Ia, and IIa. In all cases, the plane generated by six doubly bridging, two triply bridging, and two hexacoordinate oxygen donors is the reference plane from which spacings to the other nearly parallel planes (within 1.3°) have been calculated. The other four planes consist of two sets, each defined by four terminal oxo groups, four doubly bridging and a triply bridging oxygen donor, and of two sets of five vanadium centers. As shown, the most significant effect is the overall expansion of the cluster volume, reflected in the distances between the outermost layers of oxygen atoms of 4.37 Å in $[V_{10}O_{28}]^{6-}$, 4.48 Å in Ia, and 4.52 Å in IIa. The general trend in interplanar spacings reflects both changes in oxidation states and the presence of protons or alkyl substituents which remove electron density from bridging oxo groups. Comparison of the structures of $[V_{10}O_{28}]^{6-}$ and $[H_3V_{10}O_{28}]^{3-}$ indicates that protonation of three oxygens on the top oxide layer removes charge from this layer and weakens the bonds between these oxygens and the upper layer of vanadium atoms, resulting in an increase in the interplanar separation from 0.90 Å in $[V_{10}O_{28}]^{6-}$ to 0.97 Å in $[H_3V_{10}O_{28}]^{3-}$. This effect is then reflected in the reduction of charge at the central layer which causes a shortening of the interplanar spacing between the lower vanadium layer and the

---

(26) Brown, I. D.; Wu, K. K. *Acta Crystallogr., Sect. B* **1976**, *B32*, 1957.

Table III. Selected Bond Lengths (Å) and Angles (deg) for $(Et_4N)[V_{10}O_{13}\{CH_3CH_2C(CH_2O)_3\}_5]$ (II)[a]

V1–O1	2.17 (1)	V3–O17	2.03 (1)	V6–O1	2.392 (9)	V8–O8	1.78 (1)
V1–O2	2.017 (9)	V3–O20	2.00 (1)	V6–O7	2.00 (1)	V8–O9	1.973 (9)
V1–O4	1.91 (1)	V3–O23	1.590 (9)	V6–O11	2.04 (1)	V8–O26	1.60 (1)
V1–O6	2.05 (1)	V4–O1	2.042 (9)	V6–O15	2.01 (1)	V9–O2	2.25 (1)
V1–O15	1.952 (9)	V4–O2	2.01 (1)	V6–O19	1.99 (1)	V9–O5	2.08 (1)
V1–O16	1.66 (1)	V4–O3	2.046 (9)	V6–O21	1.60 (1)	V9–O6	2.105 (9)
V2–O2	2.50 (1)	V4–O5	2.06 (1)	V7–O1	2.48 (1)	V9–O12	1.98 (1)
V2–O8	1.96 (1)	V4–O17	1.947 (9)	V7–O3	2.078 (9)	V9–O13	1.974 (9)
V2–O12	2.04 (1)	V4–O18	1.93 (1)	V7–O4	2.00 (1)	V9–O27	1.58 (1)
V2–O16	2.03 (1)	V5–O1	2.39 (1)	V7–O7	1.984 (9)	V10–O1	2.29 (1)
V2–O20	1.995 (9)	V5–O10	2.00 (1)	V7–O10	2.02 (1)	V10–O5	2.059 (9)
V2–O22	1.57 (1)	V5–O14	2.00 (1)	V7–O25	1.58 (1)	V10–O6	2.052 (9)
V3–O2	2.382 (3)	V5–O18	2.022 (9)	V8–O2	2.54 (1)	V10–O11	1.95 (1)
V3–O9	2.00 (1)	V5–O19	1.99 (1)	V8–O3	2.15 (1)	V10–O14	1.95 (1)
V3–O13	2.01 (1)	V5–O24	1.58 (1)	V8–O4	1.936 (9)	V10–O28	1.61 (1)

O1–V1–O2	82.8 (4)	O9–V3–O23	101.1 (5)	O1–V6–O11	77.9 (4)	O4–V8–O8	97.0 (4)
O1–V1–O4	84.2 (4)	O13–V3–O17	89.3 (4)	O1–V6–O15	77.0 (3)	O4–V8–O9	148.8 (5)
O1–V1–O6	79.9 (4)	O13–V3–O20	87.3 (4)	O1–V6–O19	79.0 (4)	O4–V8–O26	104.7 (5)
O1–V1–O15	83.7 (4)	O13–V3–O23	101.4 (5)	O1–V6–O21	177.0 (5)	O8–V8–O9	90.9 (4)
O1–V1–O16	173.5 (5)	O17–V3–O20	158.3 (4)	O7–V6–O11	159.1 (4)	O8–V8–O26	105.5 (5)
O2–V1–O4	88.9 (4)	O17–V3–O23	100.0 (5)	O7–V6–O15	88.3 (4)	O9–V8–O26	102.1 (5)
O2–V1–O6	83.2 (4)	O20–V3–O23	101.8 (5)	O7–V6–O19	89.1 (4)	O2–V9–O5	77.2 (4)
O2–V1–O15	165.6 (4)	O1–V4–O2	86.3 (4)	O7–V6–O21	100.4 (5)	O2–V9–O6	76.6 (4)
O2–V1–O16	93.1 (4)	O1–V4–O3	89.7 (4)	O11–V6–O15	86.3 (4)	O2–V9–O12	83.8 (4)
O4–V1–O6	162.9 (4)	O1–V4–O5	84.2 (4)	O11–V6–O19	87.6 (4)	O2–V9–O13	80.8 (4)
O4–V1–O15	94.8 (4)	O1–V4–O17	174.2 (4)	O11–V6–O21	100.4 (5)	O2–V9–O27	174.6 (5)
O4–V1–O16	100.8 (5)	O1–V4–O18	88.5 (4)	O15–V6–O19	156.0 (4)	O5–V9–O6	78.9 (4)
O6–V1–O15	89.4 (4)	O2–V4–O3	88.4 (4)	O15–V6–O21	100.4 (5)	O5–V9–O12	160.4 (4)
O6–V1–O16	94.7 (5)	O2–V4–O5	83.0 (4)	O19–V6–O21	103.5 (5)	O5–V9–O13	91.7 (4)
O15--V1–O16	99.9 (4)	O2–V4–O17	87.8 (4)	O1–V7–O3	77.9 (3)	O5–V9–O27	98.5 (5)
O2–V2–O8	78.1 (4)	O2–V4–O18	172.8 (4)	O1–V7–O4	74.6 (4)	O6–V9–O12	92.1 (4)
O2–V2–O12	76.4 (4)	O3–V4–O5	169.8 (4)	O1–V7–O7	79.2 (4)	O6–V9–O13	156.9 (4)
O2–V2–O16	71.8 (4)	O3–V4–O17	90.1 (4)	O1–V7–O10	77.7 (4)	O6–V9–O27	99.5 (5)
O2–V2–O20	79.0 (4)	O3–V4–O18	96.5 (4)	O1–V7–O25	179.8 (5)	O12–V9–O13	90.1 (4)
O2–V2–O22	176.3 (4)	O5–V4–O17	95.2 (4)	O3–V7–O4	76.3 (4)	O12–V9–O27	100.1 (5)
O8–V2–O12	154.4 (4)	O5–V4–O18	91.5 (4)	O3–V7–O7	156.6 (4)	O13–V9–O27	102.8 (5)
O8–V2–O16	85.7 (4)	O17–V4–O18	97.3 (4)	O4–V7–O10	91.7 (4)	O1–V10–O5	78.3 (4)
O8–V2–O20	87.3 (4)	O1–V5–O10	80.2 (4)	O3–V7–O25	102.2 (4)	O1–V10–O6	77.1 (4)
O8–V2–O22	104.3 (5)	O1–V5–O14	77.8 (4)	O4–V7–O7	93.3 (4)	O1–V10–O11	82.1 (4)
O12–V2–O16	87.7 (4)	O1–V5–O18	77.2 (4)	O4–V7–O10	151.5 (5)	O1–V10–O14	81.3 (4)
O12–V2–O20	86.4 (4)	O1–V5–O19	78.9 (4)	O5–V7–O25	105.7 (5)	O1–V10–O28	177.2 (5)
O12–V2–O22	101.3 (5)	O1–V5–O24	178.8 (5)	O7–V7–O10	87.8 (4)	O5–V10–O6	80.7 (4)
O16–V2–O20	150.8 (4)	O10–V5–O14	157.9 (5)	O7–V7–O25	100.8 (5)	O5–V10–O11	159.2 (4)
O16–V2–O22	105.4 (5)	O10–V5–O18	88.4 (4)	O10–V7–O25	102.1 (5)	O5–V10–O14	89.3 (4)
O20–V2–O22	103.8 (5)	O10–V5–O19	88.4 (4)	O2–V8–O3	73.8 (3)	O5–V10–O28	100.0 (5)
O2–V3–O9	80.6 (4)	O10–V5–O24	100.9 (5)	O2–V8–O4	74.5 (4)	O6–V10–O11	88.2 (4)
O2–V3–O13	76.8 (4)	O14–V5–O18	86.4 (4)	O2–V8–O8	80.2 (4)	O6–V10–O14	157.5 (4)
O2–V3–O17	76.6 (3)	O14–V5–O19	87.6 (4)	O2–V8–O9	77.2 (4)	O6–V10–O28	100.5 (5)
O2–V3–O20	81.8 (4)	O14–V5–O24	101.2 (5)	O2–V8–O26	174.2 (5)	O11–V10–O14	94.6 (4)
O2–V3–O23	176.1 (5)	O18–V5–O19	156.1 (4)	O3–V8–O4	76.0 (4)	O11–V10–O28	99.3 (5)
O9–V3–O13	157.5 (4)	O18–V5–O24	102.2 (5)	O3–V8–O8	154.0 (4)	O14–V10–O28	101.0 (5)
O9–V3–O17	86.2 (4)	O19–V5–O24	101.7 (5)	O3–V8–O9	83.8 (4)		
O9–V3–O20	88.7 (4)	O1–V6–O7	81.2 (4)	O3–V8–O26	100.4 (5)		

[a] Bond lengths and angles for the three crystallographically independent $[V_{10}O_{13}\{CH_3C(CH_2O)_3\}_5]^-$ clusters of III are essentially identical to those of the anion of II and are listed in the supplementary material.

Table IV. Comparison of Interplanar Spacings (Å) in Clusters with the $\{V_{10}O_{28}\}$ Core[a]

complex	*a*	*b*	*c*
$[V_{10}O_{28}]^{6-}$	0.90	2.19	4.37
$[H_3V_{10}O_{28}]^{3-}$	0.87, 0.97[b]	2.20, 2.16[b]	4.36
$[V_{10}O_{16}\{CH_3CH_2C(CH_2O)_3\}_4]^{4-}$	0.87	2.24	4.48
$[V_{10}O_{13}\{CH_3CH_2C(CH_2O)_3\}_5]^-$	0.93	2.26	4.52

[a] See Figure 4 for definitions of *a*, *b*, and *c*. (b) In the case of $[H_3V_{10}O_{28}]^{3-}$, the first entry in each column refers to the distance from the central plane to the plane containing the protonated oxo group; the second entry is the distance from the central plane to the unprotonated or "lower" layer of oxo groups.

lower oxide layer in $[H_3V_{10}O_{28}]^{3-}$ relative to $[V_{10}O_{28}]^6$. In the cases of Ia and IIa, the oxygen donors of the trisalkoxy ligands span the central and outer oxygen layers such that the effects of replacement of oxo groups by alkoxy oxygens are effectively evenly distributed throughout the oxygen layers. The general expansion of the cluster volume as reflected in the parameter *c* is thus a consequence of the introduction of alkoxy ligands and of reduction of the V(V) centers of $[V_{10}O_{28}]^{6-}$ to V(IV) centers in Ia and IIa. As expected, the overall expansion of IIa is somewhat greater than that of Ia, relative to the parent cluster. However, the cluster expansion is relatively small, with an overall 3.5% increase in the distances between outermost oxygen layers (parameter *c*) in IIa compared to $[V_{10}O_{28}]^{6-}$. This observation concurs with recent investigations by other authors which demonstrate that vanadium clusters may accommodate significantly different ratios of reduced V(IV) sites to oxidized V(V) centers without significant structural change.[1,3]

Variable temperature solid-state magnetic susceptibility studies were performed on powdered samples of I and II in the range 4.2–300 K. Figures 5 and 6 show plots of the gram susceptibility (χ) and effective moment (μ_{eff}) per molecule.[27] The theoretical spin-only moment in the absence of coupling for a ten V(IV) d^1 system is 5.47 μ_B/molecule. The effective magnetic moment of

---

[27] Carlin, R. L. *Magnetochemistry*; Springer-Verlag: Berlin, 1986.

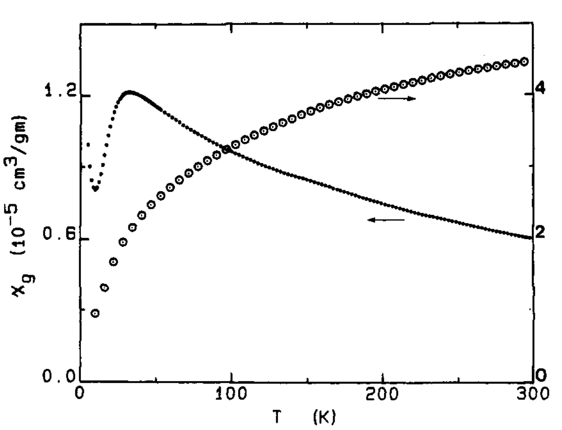

Figure 6. Plot of the magnetic susceptibility (χ_g) and effective moment (μ_{eff}) per molecule for solid II.

I at 300 K is 4.11 μ_B/molecule, indicating net antiferromagnetic exchange coupling and corresponding to 1.30 μ_B/V(IV) center. The data are distinctly nonlinear, particularly below 100 K. At high temperature, the data approach Curie–Weiss behavior, with a paramagnetic Curie temperature $\Theta = -118$ K. The effective moment of I decreases with temperature to 1.07 μ_B at 4.2 K (0.33 μ_B/V(IV) center) with a broad, shallow antiferromagnetic transition at a Nêel temperature of 18 K.

The effective magnetic moment of II at 300 K is 4.49 μ_B/molecule (1.42 μ_B/V(IV) site), again indicative of antiferromagnetic coupling. At high temperatures, the data approach Curie–Weiss behavior with $\Theta = -254$ K. The magnetic susceptibility of II increases with decreasing temperature but reaches a maximum at a Nêel temperature of 33 K, indicative of strong antiferromagnetic ordering.

The results are qualitatively similar to those observed by Müller et al.[3] for a series of V(IV)-containing clusters. In species with small numbers of V(IV) d^1 sites, the spins are trapped and separated resulting in spin-only values for μ_{eff}/V(IV). Spin–spin coupling increases with increasing numbers of V(IV) centers, such that μ_{eff}/μ_B per V(IV) values at room temperature for the "fully reduced" clusters $[V_{15}As_6O_{42}(H_2O)]^{6-}$ and $[H_4V_{18}O_{42}(I)]^{9-}$ are 1.08 and 1.06, respectively. The larger room temperature values observed for I and II appear to reflect the greater separation of V(IV) sites in these species (ca. 3.00–3.35 Å) compared to those observed for $[V_{15}As_6O_{42}(H_2O)]^{6-}$ and $[H_4V_{18}O_{423}(I)]^{9-}$ (ca. 2.80–3.05 Å).

Conclusions

Hydrothermal synthesis has been demonstrated to provide an effective method for the synthesis of poloxovanadium clusters incorporating conventional organic ligands. The marked cation dependence of the structures allows the isolation of species with different ligand to metal stoichiometries.

The clusters Ia and IIa exhibit the decavanadium core $\{V_{10}O_{28}\}$ with variable numbers of doubly and triply bridging oxo groups replaced by alkoxy oxygen donors of the trisalkoxy ligands. Although the clusters contain exclusively reduced V(IV) centers, the overall expansion of the $\{V_{10}O_{28}\}$ core relative to that of the V(V) parent cluster $[V_{10}O_{28}]^{6-}$ is relatively small.

Vanadium clusters appear to provide structures of sufficient flexibility to allow the existence of multiple oxidation states while retaining cluster integrity.

Acknowledgment. This work was supported by NSF Grant CHE9119910.

Supplementary Material Available: Tables of crystal data and experimental conditions for the X-ray studies of I–III atomic positional parameters, bond lengths, bond angles, and anisotropic temperature factors (60 pages); tables of calculated and observed structure factors (123 pages). Ordering information is given on any current masthead page.

H-Bonded Oxyhemoglobin Models with Substituted Picket-Fence Porphyrins: The Model Compound Equivalent of Site-Directed Mutagenesis

Gerald E. Wuenschell,[1] Catherine Tetreau,[2] Daniel Lavalette,[2] and Christopher A. Reed*,[1]

Contribution from the Department of Chemistry, University of Southern California, Los Angeles, California 90089-0744, and Unitê INSERM 219, Institut Curie, Biologie, Orsay, France.
Received July 26, 1991

Abstract: Iron(II) complexes of picket-fence-type porphyrins having one of the four pivalamide pickets replaced by a substituent capable of H-bonding have been synthesized as models for oxyhemoglobin. This synthetic approach is analogous to site-directed mutagenesis of the distal residues in oxygen-binding hemoproteins. Rate and equilibrium data for dioxygen binding have been determined to evaluate the effect of the H-bonding substituent and to make comparisons with more passive substituents. The effect of H-bonding on the dioxygen affinity under standard conditions (25 °C, toluene solvent, 1,2-dimethylimidazole as axial ligand) is best illustrated by the ca. 10-fold increase observed when one pivalamide substituent of picket-fence porphyrin is replaced by a phenylurea substituent. Other substituents influence dioxygen adduct stability in a variety of ways to reveal that even with an apparently straightforward systematic approach, there can be considerable difficulty in partitioning the various factors that influence O_2 affinity. This applies to both model compounds and mutant proteins.

Introduction

The present chemical understanding of how hemoglobin functions as a reversible dioxygen carrier has arisen from an exemplary interplay of protein studies and synthetic model investigations.[3] Prominent among the synthetic models is picket-fence porphyrin.[4] Its tetrapivalamide enclosure of the dioxygen binding site mimics the distal globin wrapping in hemoglobin. Once this and other necessary and sufficient conditions for re-

---

(1) University of Southern California.

(2) Institut Curie.

(3) Perutz, M. F. *Annu. Rev. Biochem.* **1979**, *48*, 327.

(4) Collman, J. P. *Acc. Chem. Res.* **1977**, *10*, 265.

0002-7863/92/1514-3346$03.00/0 © 1992 American Chemical Society